Intraslab Earthquake of 16 June 2013 (M_w 5.9), One of the Closest Such Events to Mexico City

by S. K. Singh, X. Pérez-Campos, V. H. Espíndola, V. M. Cruz-Atienza, and A. Iglesias

INTRODUCTION

Normal-faulting intraslab earthquakes in the subducted Cocos plate occur as close as 112 km from Mexico City at depths of ~50–55 km (Fig. 1). The incident wavefield in the Valley of Mexico from these earthquakes is dominated by body waves (Furumura and Singh, 2002). The stress drops of these earthquakes are relatively large (García *et al.*, 2004). In contrast, interplate earthquakes affecting the city occur along the Pacific coast of Mexico at distances greater than about 300 km and at shallower depth (~15–20 km), and they involve lower stress drops relative to intraslab earthquakes (García *et al.*, 2004). The incident waves in the valley from interplate earthquakes are dominated by *Lg* and surface waves (e.g., Campillo *et al.*, 1988). For these reasons, the character of the ground motion in the valley during the two types of earthquakes differs significantly (see e.g., Singh *et al.*, 2013), and the intraslab earthquakes are felt very strongly in the lakebed zone as well as the hill zone of the valley. These zones refer to the division of the area based on geotechnical characteristics of the subsoil. The lakebed zone comprises 30–80 m thick deposit of highly compressible, high-water-content clay underlain by resistant sands, whereas the hill zone is underlain by lava flows and volcanic tuffs. Because of extremely low shear wavespeed in the clay layer (as low as 50 m/s), the sites in the lakebed zone suffer large amplification, ~10–50, at their natural frequencies (~0.5 Hz) with respect to hill-zone sites (Singh, Lermo, *et al.*, 1988; Singh, Mena, and Castro, 1988; Reinoso and Ordaz, 1999).

The intraslab earthquake of 16 June 2013 (M_w 5.9) is the most recent example of an event that generated very intense ground motions in Mexico City. The earthquake was located in the state of Guerrero, south of University City (CU), a hill-zone site in the National Autonomous University of Mexico (UNAM) main campus, at a depth of 55 km and at an epicentral distance of 132 km (Fig. 1). It produced the second largest A_{max} (19.5 gal) and the third largest V_{max} (2.2 cm/s) in the last 50 years at CU, in which A_{max} and V_{max} are the peak acceleration and velocity, respectively. Most inhabitants of the city reported feeling the earthquake extremely strongly. Many did not believe that the magnitude of the earthquake was only 5.9; some thought that the authorities were intentionally under reporting it. According to a well-known TV news anchorman, it was "an earthquake of (magnitude) 5.8, which caused fear like one of (magnitude) 10" (Corte Informativo 1, Noticiero con Joaquín López-Dóriga, 17 June 2013; http://youtu.be/AclzrkYgwWA, last accessed January 2014). Although the earthquake caused general panic, no damage was reported in the city.

Here, we present an initial investigation of the source characteristics of the 2013 earthquake and the ground motions produced by this and other similar events and investigate whether the ground motions produced by the earthquake in Mexico City were unusual. The results of the study are relevant in understanding the reasons for the consternation that intraslab earthquakes cause in the city. They are also relevant for the estimation of seismic hazard from such events, a topic of continuing interest (e.g., Rosenblueth *et al.*, 1989; Pacheco and Singh, 1995; Singh *et al.*, 1996; Iglesias *et al.*, 2002). This study is a continuation of a previous one, which discusses at length the issue of intraslab versus interplate earthquakes as recorded in Mexico City (Singh *et al.*, 2013).

SEISMOTECTONICS OF THE REGION

Along the Guerrero segment of the Mexican subduction zone, the region of interest in this study, the oceanic Cocos plate, shows an initial shallow-angle subduction then flattens and becomes subhorizontal (Suárez *et al.*, 1990; Singh and Pardo, 1993; Pardo and Suárez, 1995; Pérez-Campos *et al.*, 2008; Pacheco and Singh, 2010). Shallow-dipping, interplate thrust events occur up to about ~65 km from the trench (~5 km inland) and reach a depth of about 25 km. Further inland, the unbending of the slab gives rise to both intraslab compressional as well as extensional earthquakes in the depth range of 25–45 km. The interface becomes horizontal at a distance of ~120 km from the trench at a depth of ~45 km. The subducted slab is devoid of seismicity in the distance range of ~105–160 km. Sparse intraslab, normal-faulting seismicity resumes at a distance of 160 km and lasts till ~250 km. No intraslab earthquake has been recorded beyond 250 km along this profile (or, equivalently, at less than 112 km epicentral distance from CU). The depths of the earthquakes in the distance range of 160–250 km are ~50–60 km. Episodic slow-slip events and nonvolcanic tremors have been documented in the region where the slab is horizontal (Kostoglodov *et al.*, 2003; Iglesias *et al.*, 2004; Payero *et al.*, 2008).

Tomographic studies suggest that the horizontal Cocos slab abruptly plunges almost vertically around 250 km from

doi: 10.1785/0220130179

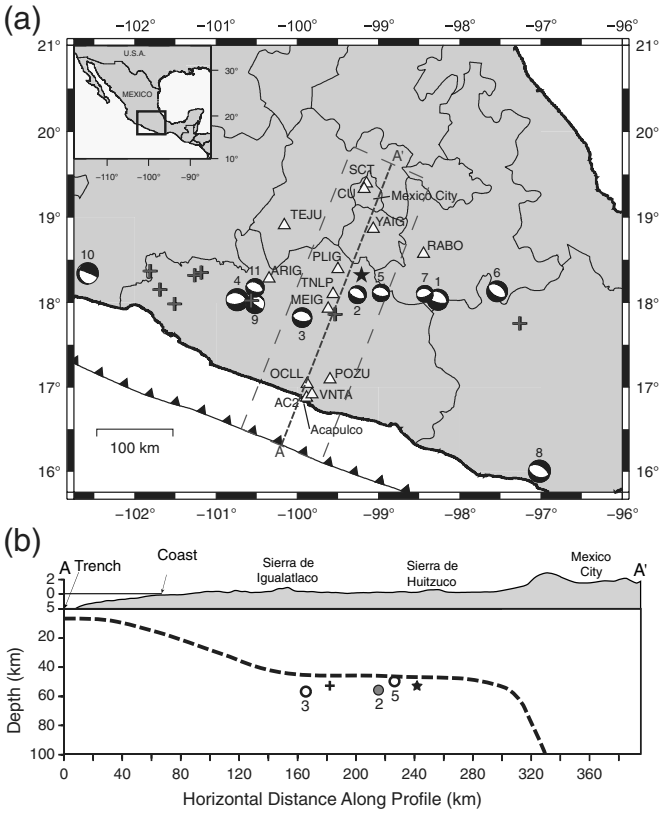

▲ **Figure 1.** (a) A tectonic map of Mexico. Focal mechanisms of the intraslab earthquakes listed in Table 2 are shown at their epicenters. The numbers are keyed to event numbers in the table. Event 2, the earthquake of 16 June 2013 (M_w 5.9), and event 11, the earthquake of 15 November 2012 (M_w 6.1), are not listed in Table 2. The plus symbols indicate the locations of the additional intraslab earthquakes that are analyzed in the study. The star indicates the earthquake of 27 October 1991 (M_w 4.6), which is the closest known intraslab earthquake to Mexico City. Triangles with names indicate the stations from which *P*-wave (*S*-wave at MEIG) seismograms of the 2013 earthquake were used to determine source directivity. (b) The cross section along A–A′, located in (a). As the geometry of the Benioff zone changes along the subduction zone, only events that fall between the two parallel dashed lines in (a) are projected onto the section. The dashed line on the section corresponds with the top of the subducted slab mapped from seismicity (Pacheco and Singh, 2010) and receiver functions and tomography (Pérez-Campos *et al.*, 2008).

the trench (Husker and Davis, 2007; Pérez-Campos *et al.*, 2008). The sparse intraslab seismicity in the horizontal segment of the slab and its abrupt end at ~250 km from the trench suggests that the plunging slab is broken off as it changes its dip (Pacheco and Singh, 2010).

SOURCE PARAMETERS

Basic source parameters of the earthquake reported by different agencies as well as those obtained in this study are listed in Table 1. The earthquake occurred in a region with reasonably dense network of broadband seismographs and accelerographs. Some of the near-source seismograms were clipped during the earthquake. Because all broadband seismographs are collocated with accelerographs, we used the strong-motion recordings at the stations where the seismograms were clipped. We note there are only minor differences in the reported seismic moments, focal mechanisms, and depths. The epicenters listed in the Global CMT catalog and the one reported by National Earthquake Information Center (NEIC; U.S. Geological Survey) are 21 km toward N38°E and 9 km toward N34°E, respectively, with respect to that obtained from local and regional *P*- and *S*-wave phase data.

SOURCE SPECTRUM AND STRESS DROP FROM NEAR-SOURCE RECORDINGS

We estimated source displacement and acceleration spectra, $\dot{M}_0(f)$ and $f^2\dot{M}_0(f)$, of the earthquake from the analysis of the *S*-wave group recorded at near-source hard sites. The method is discussed elsewhere (see e.g., García *et al.*, 2004). Here we describe it briefly. The Fourier acceleration spectral amplitude of the intense part of the ground motion at a station, under far-field, point-source approximation, may be written as

$$A(f,R) = Cf^2\dot{M}_0(f)G(f)e^{-\pi fR/\beta Q(f)}, \quad (1)$$

in which

$$C = FPR_{\theta\phi}(2\pi)^2/(4\pi\rho\beta^3); \quad (2)$$

$\dot{M}_0(f)$ is the moment rate (or source displacement) spectrum so that $\dot{M}_0(f) \to M_0$ as $f \to 0$; R is the hypocentral distance; $R_{\theta\phi}$ is the average radiation pattern (0.55); F is the free-surface amplification (2.0); P takes into account the partitioning of energy in the two horizontal components $(1/\sqrt{2})$; β and ρ are shear-wave velocity and density, respectively, in the focal region; and $Q(f)$ is the quality factor that includes both anelastic absorption and scattering. For inslab Mexican earthquakes, the appropriate geometrical spreading term $G(R)$ is R^{-1}, and the corresponding $Q(f)$ is $251f^{0.58}$ (García *et al.*, 2004). Because the depth of the earthquake (55 km) puts the focus in the upper mantle, we take $\beta = 4.68$ km/s and $\rho = 3.2$ kg/m^3. Taking logarithms of equation (1) we obtain

$$\log[A(f,R)] = \log C + \log[f^2\dot{M}_0(f)] - 1.36fR/\beta Q(f). \quad (3)$$

Equation (3) is solved for each station to obtain $\log[f^2\dot{M}_0(f)]$, and then the average is computed. Only data from known hard sites were included in the analysis, and no site effects were considered.

The source displacement and acceleration spectra of the earthquake are shown in Figure 2a. The low-frequency level of the source displacement spectrum yields seismic moment M_0 of 9.1×10^{17} N·m, which is nearly the same as reported

Table 1
Source Parameters of the Intraslab Earthquake of 16 June 2013

Origin Time (hh:mm:ss.s)	Latitude (° N)	Longitude (° W)	H (km)	M_0 (N·m)	M_w	Strike (φ)	Dip (δ)	Rake (λ)	Source
05:19:04.9	18.230	99.130	52	8.0×10^{17}	5.9	313°	35°	−70°	Global CMT
05:18:59.9	18.149	99.204	52	6.6×10^{17}	5.8	296°	23°	−80°	NEIC, USGS
05:19:03.0	18.083	99.251	56	9.3×10^{17}	5.9	328°	31°	−48	SSN*
05:19:02.0	18.100	99.270	50	8.7×10^{17}	5.9	310°	37°	−70°	UNAM, W-phase solution
05:19:02.4	18.108	99.230	55	9.1×10^{17}	5.9	–	–	–	This study†

*SSN, Servicio Sismológico Nacional. Location from local and regional P- and S-phase data, and M_0 and focal mechanism from regional moment tensor inversion.
†Location from local and regional phase data using broadband and strong-motion recordings and M_0 from S-wave spectra of local recordings.

by other sources (Table 1). We interpret the spectrum within the framework of Brune ω^2 source model (Brune, 1970) and estimate the corner frequency f_c as 0.803 Hz, the corresponding radius a of the fault as 2.2 km, and the stress drop $\Delta\sigma$ as 39.1 MPa.

Following the same procedure, we computed source spectra of four other intraslab earthquakes located within 200 km from CU: 21 July 2000, M_w 5.8, R_{CU} = 145 km; 15 November 2012, M_w 6.1, R_{CU} = 198 km; 22 May 2009, M_w 5.8, R_{CU} = 160 km; 11 December 2011, M_w 6.5, R_{CU} = 194 km (Fig. 2b–e). Except the earthquake of 15 November 2012, the other events are listed in Table 2. This table includes ten intraslab earthquakes with largest recorded A_{max} at CU in the period 1964–2013. The event of 15 November 2012 does not make the list because of its relatively small A_{max} (4.5 gal). The estimated stress drops of the four earthquakes, based on the Brune ω^2 source model, are 37.7, 41.4, 44.7, and 60 MPa, respectively. We note that spectra of the earthquakes of 2000 and 2009 are well fit by the ω^2 source model, whereas those of the 2011, 2012, and 2013 earthquakes are better characterized by a two-corner frequency model (e.g., Gusev, 1983; Boatwright and Choy, 1992; Atkinson and Boore, 1995; Boore, 2003; García *et al.*, 2004). Here we have interpreted all spectra in the framework of the ω^2 model. With the exception of the 2011 earthquake, there is no significant difference in the stress drops of the events that are only slightly greater than the median $\Delta\sigma$ of 30 MPa, as reported by García *et al.* (2004) for inslab Mexican earthquakes.

DURATION OF *P* PULSE AND SOURCE DIRECTIVITY

Near-source displacement seismograms of the 2013 earthquake reveal a unipolar P pulse, which is composed of two subevents (Fig. 3). The duration of the P pulse, T_R, varies, suggesting a directivity effect. For a rupture propagating with a velocity v_R along a fault of length L, the rupture duration T_R is given by

$$T_R = (L/v)[v/v_R - \cos\theta], \quad (4)$$

in which v is the wavespeed and θ is the angle between the direction of the rupture propagation and the direction of the ray leaving the source to reach the station. From observed values of T_R and an assumed value of v/v_R, we can estimate L because we know the focal mechanism of the earthquake, the station azimuths, and the takeoff angles. We take the nodal plane defined by azimuth φ of 313° and dip δ of 35° (Table 1) as the fault plane. For the P wave, we take $\alpha = v = 8$ km/s and consider two cases: (1) $\alpha/v_R = 3.5$, which corresponds to $v_R/\beta = 0.5$, and (2) $\alpha/v_R = 2.2$, which corresponds to $v_R/\beta = 0.78$. Case 1 is suggested by a dynamic inversion of near-source displacement seismograms of the nearby 2011 intraslab earthquake (event 3, Table 2, Fig. 1), which yields $v_R/\beta \sim 0.5$ (Díaz-Mojica *et al.*, 2013). Case 2 corresponds to the commonly accepted value of v_R/β. In the analysis, we vary the rupture direction, Γ, on the fault plane and, for each Γ, compute $\cos\theta$, hence L, at each station from equation (4) above. [See equation 4.83 of Aki and Richards (1980) for an expression for $\cos\theta$.] The value of Γ that minimizes the dispersion in L gives the rupture direction and the corresponding L is the estimated length of the rupture.

We find that for case 1, $\alpha/v_R = 3.5$ ($v_R/\beta = 0.5$), the estimated Γ is −50° and mean and median values of L are 4.1 and 3.9 km, respectively. For case 2, that is $\alpha/v_R = 2.2$ ($v_R/\beta = 0.78$), $\Gamma = -20°$, mean $L = 7.2$ km, and median $L = 7.3$ km. We note that the estimated L corresponding to case 1 is close to the source diameter of 4.4 km estimated above from the spectral analysis of S wave and Brune source model. This agreement, however, is largely fortuitous because Brune model assumes a spontaneous rupture on a circular fault and does not account for directivity.

OBSERVED AND PREDICTED A_{max} AND V_{max}

Figure 4 shows observed A_{max} and V_{max} as a function of R, along with the corresponding median and ±1 standard deviation (σ) values for an M_w 5.9 event estimated from ground-motion prediction equations (GMPEs) given by García *et al.* (2005). These GMPEs were developed from recordings of intraslab Mexican earthquakes. In the figure the observed

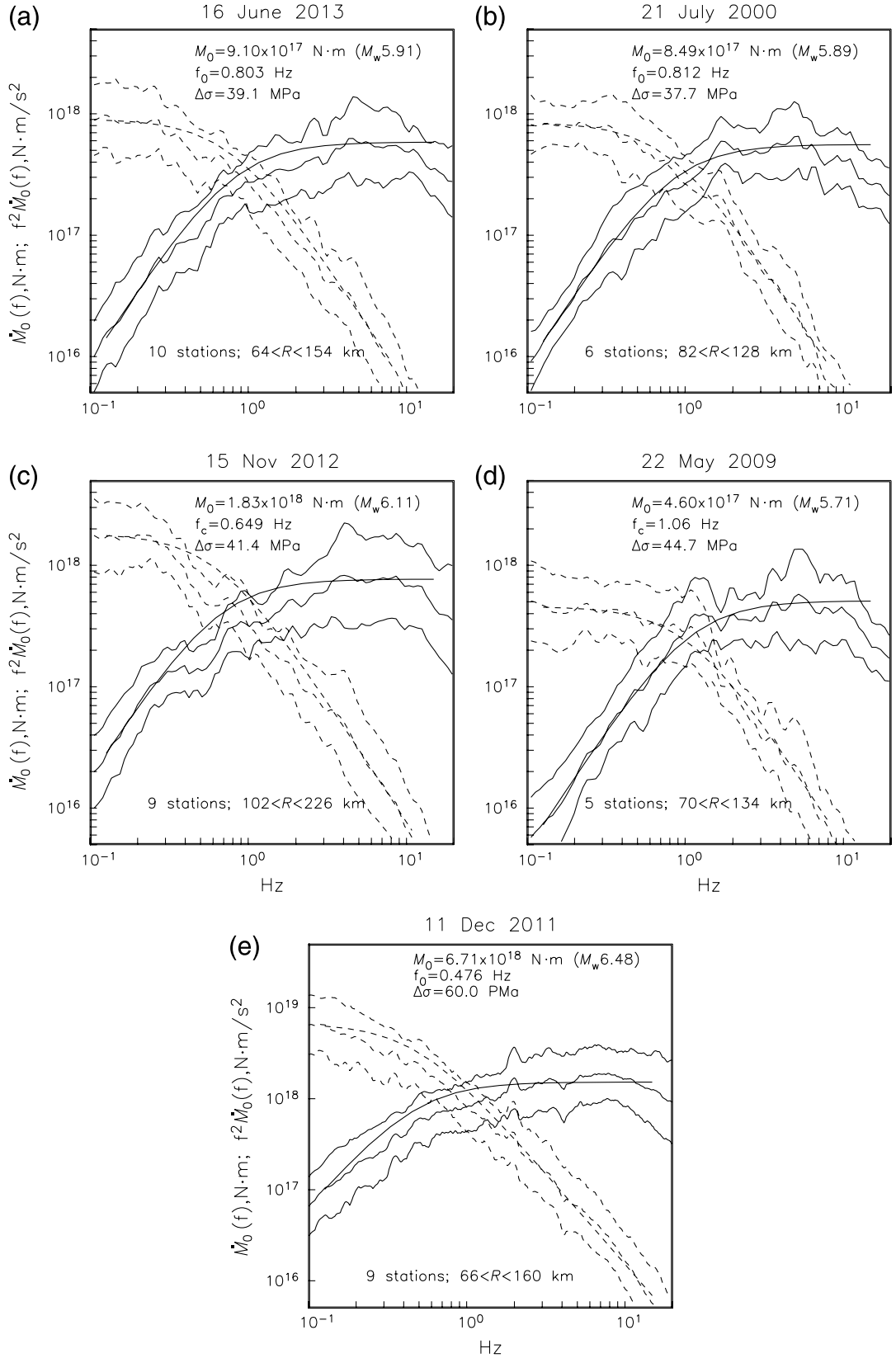

▲ **Figure 2.** Average source displacement $\dot{M}_0(f)$ and acceleration $f^2\dot{M}_0(f)$ spectra (mean and ± 1 standard deviation curves) of five intraslab earthquakes located within 200 km from CU, Mexico City. Superimposed are curves from the ω^2 source model, which fit the spectra (smooth curves). (a) 16 June 2013, M_w 5.9; (b) 21 July 2000, M_w 5.9; (c) 15 November 2012, M_w 6.1; (d) 22 May 2009, M_w 5.7; and (e) 11 December 2011, M_w 6.5. With the exception of the 2011 earthquake, the stress drop of other events is about the same.

Table 2
Ten Intraslab Earthquakes with Largest Recorded A_{max} at CU in the Period 1964–2013, Listed in Descending Order*

Event Number	Date (yyyy/mm/dd)	Latitude (°)	Longitude (°)	H (km)	m_b	M_w	R (km)	A_{max} (gal)†	V_{max} (cm/s)†
1	1980/10/24	18.03	−98.27	65	6.3	7.0	184	24.4	3.24
2	2013/06/16	18.09	−99.26	56	5.9	5.9	148	19.5	2.21
3	2011/12/11	17.82	−99.94	57	6.2	6.5	194	19.2	1.40
4	1964/07/06	18.03	−100.74	55	6.5	7.3	221	17.1	1.82
5	2000/07/21	18.11	−98.97	50	5.4	5.8	145	12.8	0.82
6	1999/06/15	18.13	−97.54	60	6.4	6.9	225	11.6	1.84
7	2009/05/22	18.10	−98.43	46	5.8	5.6	160	8.6	0.66
8	1999/09/30	16.00	−97.02	47	6.5	7.4	433	7.8	2.32
9	1994/12/10	17.98	−100.52	50	6.5	6.4	212	5.8	0.91
10	1997/01/11	18.34	−102.58	40	6.5	7.1	378	5.1	1.99

*The intraslab earthquake of 28 August 1973 (M_w 7.0, R = 311 km) is not listed because it was not recorded at CU, probably due to instrumental malfunction. The estimated A_{max} is 9.3 gal (Singh *et al.*, 2013). Local earthquakes are excluded.
†$A_{max} = [(A_n^2 + A_e^2)/2]^{1/2}$; $V_{max} = [(V_n^2 + V_e^2)/2]^{1/2}$

values at CU are shown by a different symbol. The observations and predictions are in reasonable agreement except at CU, where the observed V_{max} is abnormally high (~7.5 times the predicted median value). We recall that CU was not included in the regression analysis of García *et al.* (2005) because of suspected site effect (Ordaz and Singh, 1992; Singh *et al.*, 1995). Hence, an anomalously large V_{max} at CU is not a surprise. In the next section, we investigate whether it was only due to the site effect or the source directivity, documented above, also played a role. To this end, we next analyze strong-motion recordings of intraslab earthquakes at CU.

GROUND MOTION AT CU, MEXICO CITY

An accelerometric station has been continuously operating at CU since 1964. This site may be considered a representative hill-zone site. It has been taken as the reference site in computing amplification at lakebed sites (e.g., Singh, Lermo, *et al.*, 1988; Singh, Mena, and Castro, 1988; Reinoso and Ordaz, 1999). The quality of accelerograph at CU has improved with time so that all recent events are currently well recorded if the peak acceleration exceeds ~2 gal. However, for the entire period, 1964–2013, the data set is complete only for events with $A_{max} \geq 6$ gal (Singh *et al.*, 2013). (An exception is the intraslab earthquake of 28 August 1973 [M_w 7.0, R = 311 km], which was not recorded at CU, probably due to instrumental malfunction.) Table 2 lists ten intraslab earthquakes with largest recorded A_{max} at CU in the period 1964–2013. Here $A_{max} = [(A_n^2 + A_e^2)/2]^{1/2}$, and A_n and A_e are peak ground accelerations in the north–south and east–west directions, respectively. The table also gives the corresponding values of V_{max}. We note that A_{max} and V_{max} at CU during the 2013 earthquake, 19.5 gal and 2.2 cm/s, respectively, were the second and the third largest. This may explain why the earthquake was felt so strongly in Mexico City.

Figure 5a shows median Fourier acceleration spectrum of the two horizontal components recorded at CU of five intraslab earthquakes ($5.6 \leq M_w \leq 6.5$) with $R_{CU} < 200$ km, including the 2013 earthquake. Except for the 15 November 2012 earthquake (M_w 6.1, m_b 5.7, R_{CU} = 196 km), which gave rise to A_{max} of only 4.5 gal at CU, all others are listed in Table 2. We note that the spectral level of the 2013 earthquake at CU is greater than those of the earthquakes of 2009 (M_w 5.6), 2000 (M_w 5.8), and 2012 (M_w 6.1) in the frequency band of 0.2–8.0 Hz, as is its A_{max} of 19.5 gal. The spectral amplitudes of the 11 December 2011 earthquake (M_w 6.5; R_{CU} = 194 km), as compared to those of the 2013 earthquake, are greater for $f < 0.4$ Hz, smaller for $0.4 < f < 2.0$ Hz, and greater, again, for $f > 2.0$ Hz. A_{max} of the 2011 earthquake, 19.2 gal, is only slightly smaller than that of the 2013 event. To understand whether the spectral differences are due to distance or source effect, we reduced the observed spectra at CU to a common source distance, R, of 150 km using equation (1). The result is illustrated in Figure 5b. The spectral level of the 2013 earthquake is greater than those of events with comparable or smaller magnitudes (M_w 5.6, 5.8, 6.1) for $0.3 < f < 8.0$ Hz. It is, however, exceeded by the spectrum of the 2011 earthquake except near 1 Hz. The magnitude (M_w 6.5) and stress drop (60 MPa) of the 2011 earthquake are also significantly larger. In as much as the estimated Brune stress drops of ~M_w 6.0 events are about the same, this suggests that the relatively high spectral level of the 2013 earthquake at CU is most probably due to the directivity effect. The spectral level at ~1 Hz of the 2013 earthquake is nearly equal to that of the 2011 earthquake but is much greater than that of the other three earthquakes in Figure 5b. The m_b values of the 2013 and 2011 events are 5.9 and 6.2, respectively; those of the others events are 5.4, 5.7, and 5.8. This, again, suggests that energy radiation at CU near 1 Hz was anomalous probably as a consequence of directivity.

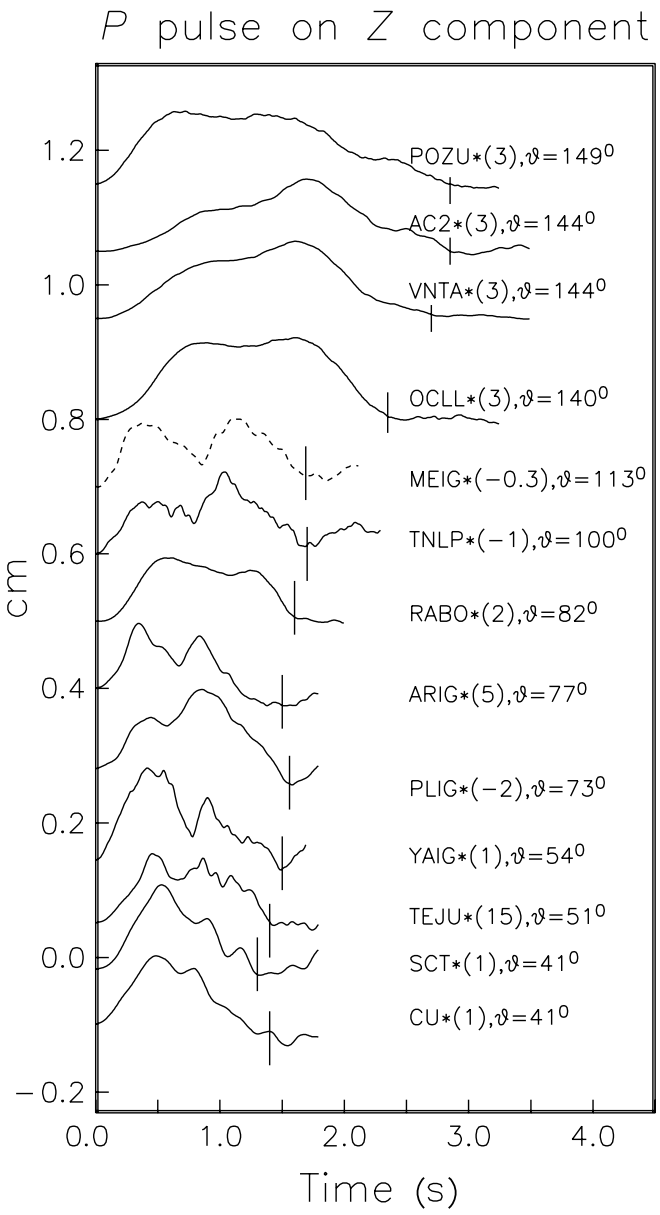

▲ **Figure 3.** *P*-wave displacement pulse on the *Z* component at near-source stations. At MEIG, the *S* pulse on the north–south component is shown. The number following the station name indicates the factor by which the *P*-wave amplitudes have been multiplied. The traces are ordered according to θ, the angle between the direction of the rupture on the fault plane (Γ) and the ray leaving the source to the station corresponding to the case $\alpha/v_R = 3.5$ ($v_R/\beta = 0.5$). In this case, rupture direction is estimated as $\Gamma = -50°$ (see text).

An alternative way to investigate whether ground motion in CU during the 2013 earthquake was unusually large is to compare observed A_{max} and V_{max} at the site during events listed in Table 2 with the predictions from GMPEs. Figure 6a–c shows $\log(A_{max}^{obs}/A_{max}^{cal})$ as a function A_{max}, M_w, and R, respectively. In the figures we have added the earthquake of 15 November 2012 (identified as event number 11) and nine other intraslab earthquakes that are not listed in

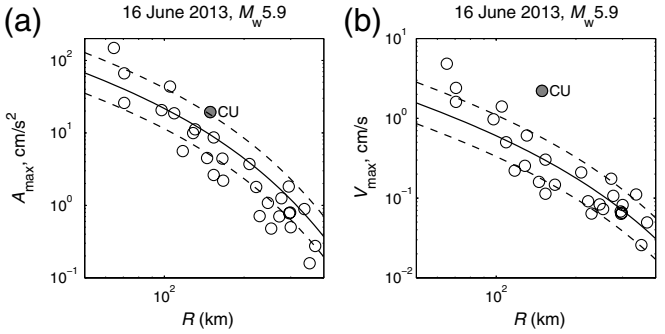

▲ **Figure 4.** (a) A_{max} versus R plot for 15 June 2013 earthquake. (b) V_{max} versus R plot. Observed values at CU are marked. Predicted mean ± one standard deviation curves from the GMPEs of García *et al.* (2005) are shown by curves.

Table 2. The corresponding plots for V_{max} are illustrated in Figure 6d–f. Observed A_{max} and V_{max} at CU during events 8 and 10 were relatively large. These intraslab earthquakes were located near the coast, more than 370 km from CU (Fig. 1, Table 2), just below or near the down-dip edge of the coupled plate interface where large/great shallow-dipping thrust earthquakes occur (Singh *et al.*, 2000; Santoyo *et al.*, 2005). They were also somewhat shallower than the other intraslab earthquakes that were located further down-dip. Relatively high A_{max} and V_{max} during these two earthquakes may be a consequence of a different crustal structure involved in the wave propagation to Mexico City and shallower depth of the sources, both factors leading to less attenuation of high-frequency ground motion than expected from the intraslab GMPEs. As to the other events in Figure 6a–c, we note that the observed A_{max} are, generally, within ± one standard deviation of the predicted ones. This suggests that the amplification of A_{max} at CU due to site effect is not large. On the other hand, the observed V_{max} exceed + one standard deviation for most events. Thus, the site effect appears more pronounced for V_{max} than for A_{max}. For the 2013 earthquake, the observed V_{max} is ~7.5 times greater than the estimated value from the GMPE; only events 8 and 10 have larger values relative to the estimated ones. We conclude that the site effect during intraslab earthquakes at CU at frequencies associated with V_{max} is significantly larger than at frequencies related to A_{max}. Furthermore, significantly large relative V_{max} for the 2013 earthquake suggests that source directivity also contributed to the anomalously high value.

THE EARTHQUAKE IN THE CONTEXT OF INTRASLAB VERSUS INTERPLATE EARTHQUAKES AS RECORDED IN MEXICO CITY

A previous study (Singh *et al.*, 2013) discussed the characteristics of the ground motion during intraslab and interplate earthquakes at CU, the representative hill-zone site, and at Secretaría de Comunicaciones y Transportes (SCT), a typical lakebed zone site. The ratios of A_{max} and A_{max}^{HF} at the two sites

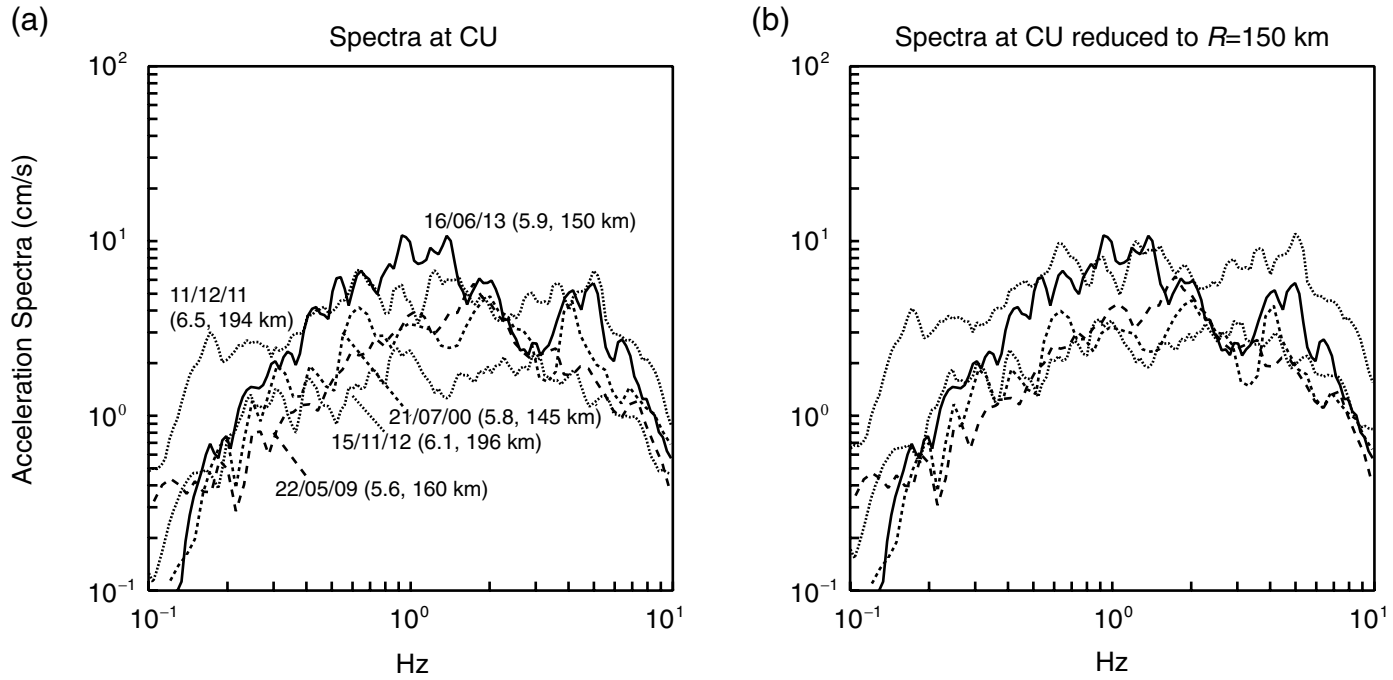

▲ **Figure 5.** (a) Fourier acceleration spectra at CU of five intraslab events ($5.6 \le M_w \le 6.5$; $145 \le R \le 194$), including the 2013 earthquake. (b) The spectra shown in (a), reduced to a common hypocentral distance R of 150 km (see text).

were used as metrics for this purpose, in which A_{max}^{HF} is the high-frequency A_{max} computed from band-pass filtered (2.5–8.5 Hz) accelerograms. Figure 7, modified from Singh *et al.* (2013), summarizes the results: (a) A_{max}^{HF}/A_{max} at CU is between 0.6 and 0.9 for the intraslab earthquakes, much larger than for the interplate ones (Fig. 7a). (b) A_{max}^{HF}/A_{max} at SCT for both types of earthquakes are relatively small and decays with R (Fig. 7b). (c) $A_{max}(SCT)/A_{max}(CU)$ depends on R so that $A_{max}(SCT)/A_{max}(CU) = 0.01R - 0.39$ ($\sigma = 0.29$). (d) $A_{max}^{HF}(SCT)/A_{max}^{HF}(CU)$ for intraslab earthquakes (generally < 1) is independent of R. The ratio is too scattered for interplate earthquakes to establish any trend (Fig. 7d). As discussed in Singh *et al.* (2013), the ground-motion characteristics summarized in Figure 7 may be explained by noting that, with respect to interplate earthquakes, (1) the incident waves from intraslab events differ, (2) the intraslab events generally occur closer to Mexico City, and (3) the stress drops during intraslab earthquakes are greater.

During the 2013 earthquake, A_{max} and A_{max}^{HF} at CU were 19.5 and 12.5 gal, respectively. The corresponding values at SCT were 25.9 and 13.4 gal. It is reassuring to note that the ratios for this earthquake, plotted in the figure, follow the trend reported in the previous study. Figure 7 summarizes the difference in the gross characteristics of the ground motion to be expected in the hill and lakebed zones of Mexico City during intraslab and interplate earthquakes.

DISCUSSION AND CONCLUSIONS

The intraslab earthquake of 16 June 2013 was one of the closest such events to occur near Mexico City. Its hypocentral distance to CU, R_{CU}, was 148 km; only the following two other intraslab earthquakes are known to have been closer: 21 July 2000, M_w 5.8, $R_{CU} = 145$ km and 27 October 1991, M_w 4.4, $R_{CU} = 120$ km (Fig. 1). The 2013 earthquake produced second largest A_{max} and third largest V_{max} at CU during an intraslab earthquake since 1964 (Table 2). In the same period, only one interplate earthquake, the catastrophic 1985 Michoacan event, had a higher A_{max} (29.8 gal) at CU (see Table 1, Singh *et al.*, 2013). It is not surprising, then, that the earthquake was felt very strongly in the city and caused general panic.

The stress drop estimated from the spectral analysis of S waves is 39 MPa, about the same as the median stress drop of 30 MPa reported for intraslab earthquakes in Mexico. Yet the ground motions at CU were anomalously large, especially V_{max}. This was, most likely, a consequence of source directivity toward CU, which is clearly visible in the P pulse. Our estimate of rupture length from spectral analysis and the study of source directivity is ~4–7 km.

Mexican seismologists will do well to remember A_{max} and V_{max} values produced by previous significant intraslab and interplate earthquakes at CU (Table 2; table 1 in Singh *et al.*, 2013) in order to put ground motions from future earthquakes in proper perspective and, hence, to better communicate with the public. It will also be useful to keep in mind that the exceedance rate of A_{max} at CU from interplate and intraslab earthquakes is about the same (Singh *et al.*, 2013). In spite of similar exceedance rate of A_{max}, historically, the interplate earthquakes have been far more damaging than the intraslab ones. This, no doubt, reflects the difference in the ground-motion characteristics and the duration of intense motion during the two types of events.

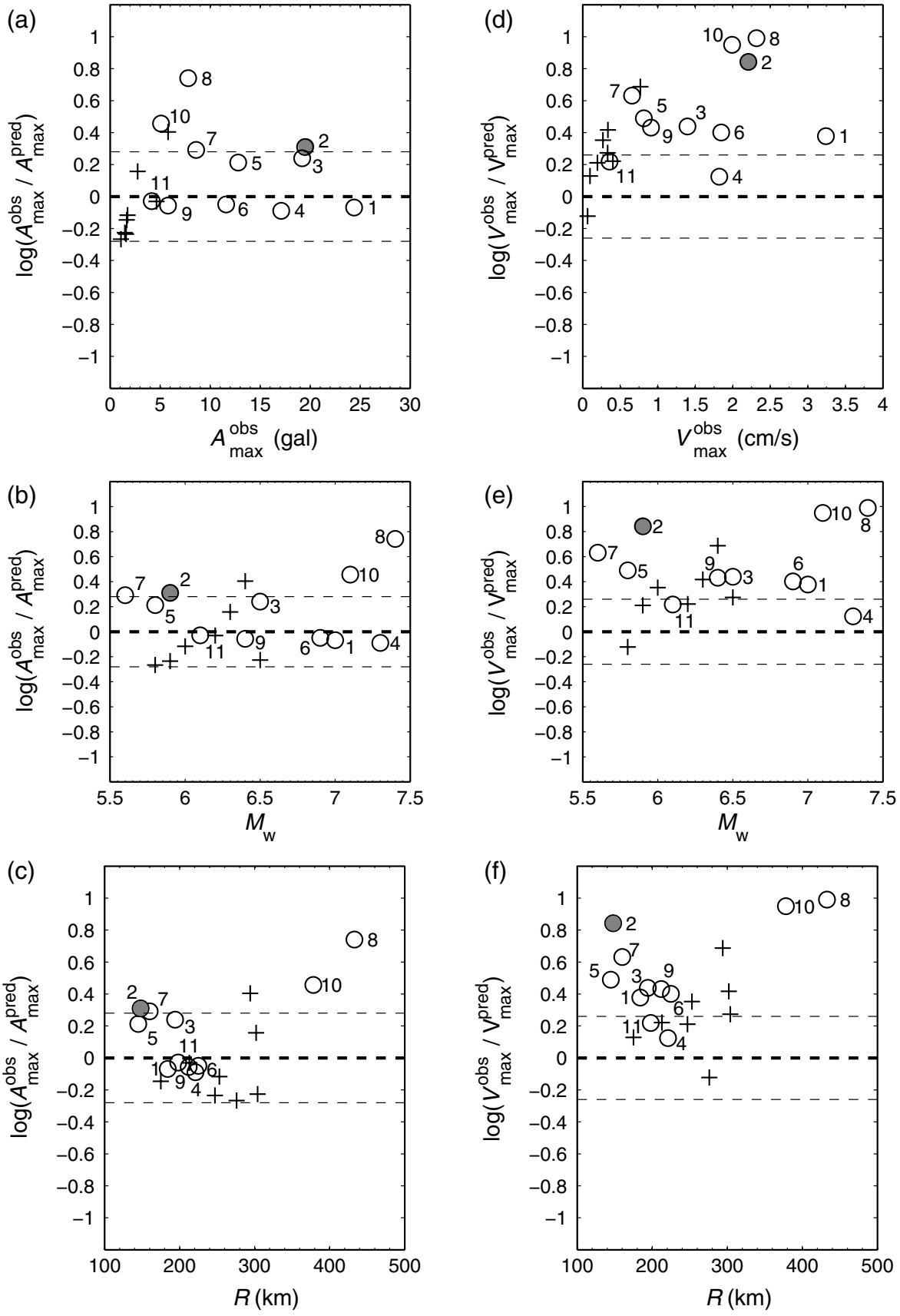

▲ **Figure 6.** (Observed/predicted) A_{max} at CU for the 10 events listed in Table 2 plus event 11 (15 November 2012) and nine additional intraslab earthquakes plotted as a function of (a) A_{max}, (b) M_w, and (c) R. The corresponding plots for V_{max} are shown in (d), (e), and (f).

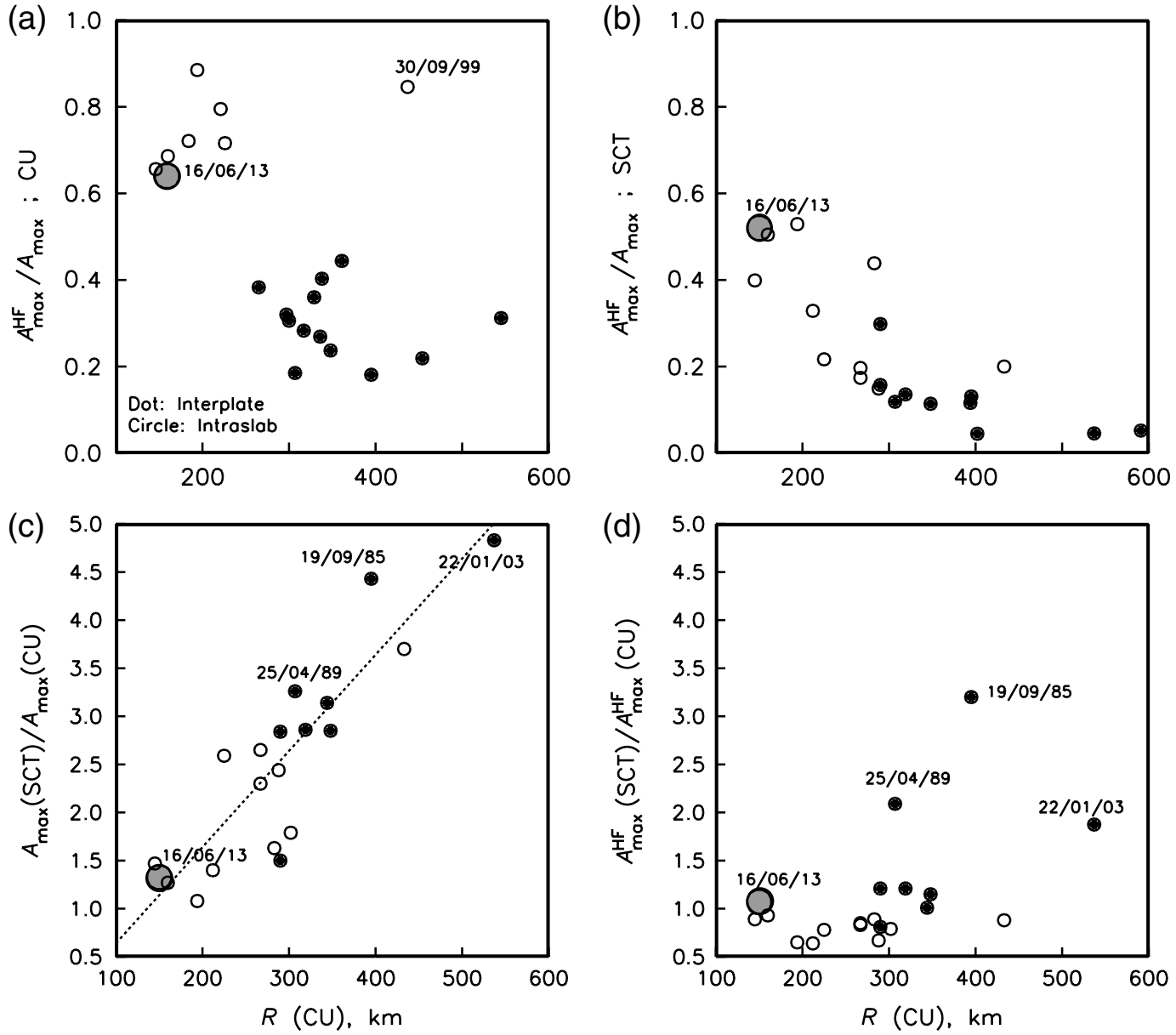

▲ **Figure 7.** Ground-motion parameters recorded at CU and SCT during interplate and intraslab earthquakes (modified from Singh *et al.*, 2013). (a) A^{HF}_{max}/A_{max} at CU as a function of R. (b) A^{HF}_{max}/A_{max} at SCT as a function of R. (c) $A_{max}(SCT)/A_{max}(CU)$ as a function of R. The least-square fit, $A_{max}(SCT)/A_{max}(CU) = 0.01R - 0.39$, is shown by the dashed line. (d) $A^{HF}_{max}(SCT)/A^{HF}_{max}(CU)$ as a function of R. The earthquake of 16 June 2013 follows the trend of intraslab earthquakes.

ACKNOWLEDGMENTS

We acknowledge efforts of the technicians of Instituto de Geofísica and Instituto de Ingeniería who are responsible for the operation of UNAM's seismic and strong-motion networks. We thank the reviewers and associate editor for their comments. Rosario Delgado and Citlali Pérez kindly provided us with several strong-motion recordings analyzed in this study. The research was partially supported by DGAPA, UNAM projects IN111411-2 and IN111314.

REFERENCES

Aki, K., and P. G. Richards (1980). *Quantitative Seismology*, Vol. 1, W.H. Freeman and Co., San Francisco, California, 557 pp.

Atkinson, G. M., and D. M. Boore (1995). New ground motion relations for eastern North America, *Bull. Seismol. Soc. Am.* **85,** 17–30.

Boatwright, J., and G. Choy (1992). Acceleration source spectra anticipated for large earthquakes in northeastern North America, *Bull. Seismol. Soc. Am.* **82,** 660–675.

Boore, D. M. (2003). Simulations of ground motion using the stochastic method, *Pure Appl. Geophys.* **160,** 635–675.

Brune, J. N. (1970). Tectonic stress and the spectra of seismic shear waves from earthquakes, *J. Geophys. Res.* **75,** 4997–5009.

Campillo, M., P.-Y. Bard, F. Nicollin, and F. Sánchez-Sesma (1988). The Mexico earthquake of September 19, 1985—The incident wavefield in Mexico City during the great Michoacán earthquake and its interaction with the deep basin, *Earthq. Spectra* **4,** 591–608.

Díaz-Mojica, J., V. M. Cruz-Atienza, R. Madariaga, S. K. Singh, J. Tago, and A. Iglesias (2013). Dynamic source inversion of the *M* 6.5 intraslab Zumpango earthquake in central Mexico: A new parallel genetic algorithm, *J. Geophys. Res.* (submitted).

Furumura, T., and S. K. Singh (2002). Regional wave propagation from Mexican subduction zone earthquakes: The attenuation functions for interplate and inslab events, *Bull. Seismol. Soc. Am.* **92,** 2110–2125.

García, D., S. K. Singh, M. Herráiz, M. Ordaz, and J. F. Pacheco (2005). Inslab earthquakes of central Mexico: Peak ground-motion parameters and response spectra, *Bull. Seismol. Soc. Am.* **95,** 2272–2282.

García, D., S. K. Singh, M. Herráiz, J. F. Pacheco, and M. Ordaz (2004). Inslab earthquakes of central Mexico: Q, source spectra and stress drop, *Bull. Seismol. Soc. Am.* **94,** 789–802.

Gusev, A. A. (1983). Descriptive statistical model of earthquake source radiation and its application to an estimation of short-period strong motion, *Geophys. J. Roy. Astron. Soc.* **74,** 787–808.

Husker, A., and P. M. Davis (2009). Tomography and thermal state of the Cocos plate subduction beneath Mexico City, *J. Geophys. Res.* **114,** doi: 10.1029/2008JB006039.

Iglesias, A., S. K. Singh, A. R. Lowry, M. Santoyo, V. Kostoglogov, K. M. Larson, and S. I. Franco-Sanchéz (2004). The silent earthquake of 2002 in the Guerrero seismic gap, Mexico ($M_w = 7.6$): Inversion of slip on the plate interface and some implications, *Geofis. Int.* **43,** 309–317.

Iglesias, A., S. K. Singh, J. F. Pacheco, and M. Ordaz (2002). A source and wave propagation study of the Copalillo, Mexico earthquake of 21 July, 2000 ($M_w = 5.9$): Implications for seismic hazard in Mexico City from inslab earthquakes, *Bull. Seismol. Soc. Am.* **92,** 885–895.

Kostoglodov, V., S. K. Singh, J. A. Santiago, S. I. Franco, K. M. Larson, A. R. Lowry, and R. Bilham (2003). A large silent earthquake in the Guerrero seismic gap, Mexico, *Geophys. Res. Lett.* **30,** 1807, doi: 10.1029/2003GL017219.

Ordaz, M., and S. K. Singh (1992). Source spectra and spectral attenuation of seismic waves from Mexican earthquakes, and evidence of amplification in the hill zone of Mexico City, *Bull. Seismol. Soc. Am.* **82,** 24–43.

Pacheco, J. F., and S. K. Singh (1995). Estimation of ground motions in the Valley of Mexico from normal-faulting, intermediate-depth earthquakes in the subducted Cocos plate, *Earthq. Spectra* **11,** 233–247.

Pacheco, J. F., and S. K. Singh (2010). Seismicity and state of stress in Guerrero segment of the Mexican subduction zone, *J. Geophys. Res.* **115,** no. B01303, doi: 10.1029/2009JB006453.

Pardo, M., and G. Suárez (1995). Shape of the subducted Rivera and Cocos plates in southern Mexico: Seismic and tectonic implications, *J. Geophys. Res.* **100,** 12,357–12,373.

Payero, J., V. Kostoglodov, N. Shapiro, T. Mikumo, A. Iglesias, X. Pérez-Campos, and R. Clayton (2008). Non-volcanic tremor observed in the Mexican subduction zone, *Geophys. Res. Lett.* **35,** L07305, doi: 10.1029/2007GL032877.

Pérez-Campos, X., Y. H. Kim, A. Husker, P. M. Davis, R. W. Clayton, A. Iglesias, J. F. Pacheco, S. K. Singh, V. C. Manea, and M. Gurnis (2008). Horizontal subduction and truncation of the Cocos plate beneath central Mexico, *Geophys. Res. Lett.* **35,** L18303, doi: 10.1029/2008GL035127.

Reinoso, E., and M. Ordaz (1999). Spectral ratios for Mexico City from free-field recordings, *Earthq. Spectra* **15,** 273–296.

Rosenblueth, E., M. Ordaz, F. J. Sánchez-Sesma, and S. K. Singh (1989). Design spectra for Mexico's Federal District, *Earthq. Spectra* **5,** 258–272.

Santoyo, M., S. K. Singh, and T. Mikumo (2005). Source process and stress change associated with the 11 January, 1997 ($M_w = 7.1$) Michoacan, Mexico, inslab earthquake, *Geofis. Int.* **44,** 317–330.

Singh, S. K., and M. Pardo (1993). Geometry of the Benioff Zone and state of stress in the overriding plate in Central Mexico, *Geophys. Res. Lett.* **20,** 1483–1486.

Singh, S. K., J. Lermo, T. Domínguez, M. Ordaz, J. M. Espinosa, E. Mena, and R. Quaas (1988). A study of relative amplification of seismic waves in the valley of Mexico with respect to a hill zone site (CU), *Earthq. Spectra* **4,** 653–674.

Singh, S. K., E. Mena, and R. Castro (1988). Some aspects of source characteristics of 19 September 1985 Michoacan earthquake and ground motion amplification in and near Mexico City from the strong motion data, *Bull. Seismol. Soc. Am.* **78,** 451–477.

Singh, S. K., M. Ordaz, and L. E. Pérez-Rocha (1996). The great Mexican earthquake of 19 June 1858: Expected ground motions and damage in Mexico City from a similar future event, *Bull. Seismol. Soc. Am.* **86,** 1655–1666.

Singh, S. K., M. Ordaz, L. Alcántara, N. Shapiro, V. Kostoglodov, J. F. Pacheco, S. Alcocer, C. Gutiérrez, R. Quaas, T. Mikumo, and E. Ovando (2000). The Oaxaca earthquake of September 30, 1999 ($M_w = 7.5$): A normal faulting event in the subducted Cocos plate, *Seismol. Res. Lett.* **71,** 67–78.

Singh, S. K., M. Ordaz, X. Pérez-Campos, and A. Iglesias (2013). Intraslab versus interplate earthquakes as recorded in Mexico City: Implications for seismic hazard, *Earthq. Spectra*, doi: 10.1193/110612EQS324M.

Singh, S. K., R. Quaas, M. Ordaz, F. Mooser, D. Almora, M. Torres, and R. Vásquez (1995). Is there truly a "hard" site in the Valley of Mexico? *Geophys. Res. Lett.* **22,** 481–484.

Suárez, G., T. Monfret, G. Wittlinger, and C. David (1990). Geometry of subduction and depth of the seismogenic zone in the Guerrero gap, Mexico, *Nature* **345,** 336–338.

S. K. Singh
X. Pérez-Campos
V. M. Cruz-Atienza
A. Iglesias
Instituto de Geofísica
Universidad Nacional Autónoma de México
Circuito de la Investigación s/n
Ciudad Universitaria, Coyoacán 04510
México City, Mexico
krishnamex@yahoo.com

V. H. Espíndola
Servicio Sismológico Nacional
Universidad Nacional Autónoma de México
Circuito de la Investigación s/n
Ciudad Universitaria, Coyoacán 04510
México City, Mexico